Featured in Physics

Decay Rate of the Nuclear Isomer ^{229}Th$(3/2^+, 7.8\ \mathrm{eV})$ in a Dielectric Sphere, Thin Film, and Metal Cavity

E. V. Tkalya[1,2,3,*]

[1]Skobeltsyn Institute of Nuclear Physics Lomonosov Moscow State University, Leninskie gory, Moscow 119991, Russia
[2]Nuclear Safety Institute of RAS, Bol'shaya Tulskaya 52, Moscow 115191, Russia
[3]National Research Nuclear University MEPhI, Kashirskoe shosse 31, Moscow 115409, Russia

(Received 16 June 2017; revised manuscript received 31 January 2018; published 21 March 2018)

The main decay channels of the anomalous low-energy $3/2^+(7.8 \pm 0.5\ \mathrm{eV})$ isomeric level of the ^{229}Th nucleus, namely the γ emission and internal conversion, inside a dielectric sphere, dielectric thin film, and conducting spherical microcavity are investigated theoretically, taking into account the effect of media interfaces. It is shown that (1) the γ decay rate of the nuclear isomer inside a dielectric thin film and dielectric microsphere placed in a vacuum or in a metal cavity can decrease (increase) in dozen of times, (2) the γ activity of the distributed source as a function of time can be nonexponential, and (3) the metal cavity, whose size is of the order of the radiation wavelength, does not affect the probability of the internal conversion in ^{229}Th, because the virtual photon attenuates at much shorter distances and the reflected wave is very weak.

DOI: 10.1103/PhysRevLett.120.122501

The change of the spontaneous emission probability of atoms and molecules due to electromagnetic boundary conditions was first predicted by Purcell in 1946 [1]. At present, this phenomenon is well studied both theoretically [2–7] and experimentally (see for example [8–12]). In nuclear physics, a similar effect was observed in the nuclear forward scattering process at the $^{57}\mathrm{Fe}(3/2^-, 14.4\ \mathrm{keV})$ nuclear level [13]. However, it is difficult to observe the Purcell effect in the decay of nuclear states since energies of nuclear transitions are large in comparison with optical atomic transitions, and penetrating γ radiation is practically not reflected at the boundary of two different media, and also, the dominant decay channel of the low energy nuclear states is internal conversion (IC), rather than γ radiation.

Nevertheless, there is one exception. As early as 1976, Kroger and Reich established the existence of a low-lying nuclear excited state with the spin $3/2^+$ in ^{229}Th through the γ ray spectroscopy following the α decay of ^{233}U [14]. In 1990, Reich and Helmer analyzed, in detail, the energies and intensities of γ transitions in the ^{229}Th in a similar experiment, found that the first excited state in ^{229}Th has an extremely low energy of $E_{\mathrm{is}} = 1 \pm 4$ eV [15]. Four years later, the energy range was narrowed to $E_{\mathrm{is}} = 3.5 \pm 1.0$ eV [16]. In spite of this, precise measurements by Beck *et al.* [17] performed in 2007 yielded $E_{\mathrm{is}} = 7.8 \pm 0.5$ eV. The latest data [18], based on the direct detection of the IC electrons, result in $6.3\ \mathrm{eV} \le E_{\mathrm{is}} \le 18.3\ \mathrm{eV}$.

Since its discovery, the low-lying $3/2^+$ nuclear state in ^{229}Th has attracted great interest of researchers. A number of limitations on the possible values of its energy and half-life was established in works [19–23]. The most detailed conditions of this kind were obtained in [24] by the direct excitation of the ^{229}Th nuclei and the detection of photons in a crystal with a large band gap (this effect was predicted in [25,26]). Nowadays several promising crystals have been found and studied intensively [27–30]. Another popular trend is to use ion traps [31–33]. Here, it is worth mentioning the highly effective excitation of the thorium isomer through the inverse electronic bridge, which was first proposed in [34] and studied later in [35].

The most important applications for all of these studies are possibly the creation of a laser working on the nuclear transition [36], and a high precision nuclear clock [31,33,37,38]. The successful implementation of these two points will lead to a technological breakthrough with far-reaching consequences for various fields of science and technology. Among the interesting possibilities, one can note the relative effects of the variation of the fine structure constant e^2 and the strong interaction parameter $m_q/\Lambda_{\mathrm{QCD}}$ [39], the inversion of the sublevels and decay of the ground state of the nucleus into the isomeric state in the muonic atom ^{229}Th [40], the α decay of the low-lying level [41] and the acceleration of the ^{229}Th nucleus α decay rate by laser radiation, and some other applications.

In this Letter, we study the change in the decay rate of the first excited state of the ^{229}Th nucleus when electromagnetic boundary conditions are applied to the studied system. Since for the photon energy range $\omega = E_{\mathrm{is}} = 7.8 \pm 0.5$ eV there exist transparent crystals and metals effectively reflecting the radiation with the wavelength $\lambda = 2\pi/\omega \approx 160$ nm (here and below we use the system of units with $\hbar = c = 1$), it should be possible for the first time to

 © 2018 American Physical Society

control the decay of a nuclear state in the same way as in the case of optical atomic transitions [8,9]. Here we consider the following four cases of the ^{229}Th isomer decay: (a) in a dielectric sphere surrounded by vacuum, (b) in a dielectric sphere placed in a metal cavity. (c) in a dielectric thin film deposited on a semiconductor, and (d) in a spherical metallic microcavity. In the cases (a), (b), and (c), the γ radiation is considered in a large band gap dielectric, where the IC is forbidden [25,26]. In the case of (d), we are concerned with the effect of the reflecting spherical metal surface on the IC process.

Gamma emission in the dielectric sphere.—The nuclear transition current $\mathbf{J}(t,\mathbf{r}') = e^{-i\omega t}\mathbf{J}(\mathbf{r}')$ creates a vector potential $\mathbf{A}(t,\mathbf{r}') = e^{-i\omega t}\mathbf{A}(\mathbf{r}',k)$, in which the field $\mathbf{A}(\mathbf{r}',k)$ obeys the equation $(\Delta_{r'}+k^2)\mathbf{A}(\mathbf{r}',k) = -4\pi\mathbf{J}(\mathbf{r}')$, where $k=\sqrt{\varepsilon}\omega$, and ε is the dielectric constant of the medium. (In the following, the field in the region of space with the permittivity $\varepsilon_{1(2)}$ will be denoted by the wave number index $k_{1(2)} = \sqrt{\varepsilon_{1(2)}}\omega$.) The solution to this equation in the region occupied by the dielectric sphere can be written in the form

$$\mathbf{A}(\mathbf{r},k_1) = \int [\mathcal{D}(\mathbf{r},\mathbf{r}',k_1) + \tilde{\mathcal{D}}(\mathbf{r},\mathbf{r}',k_1)]\mathbf{J}(\mathbf{r}')d^3r', \qquad (1)$$

where the Green function obeys the inhomogeneous Helmholtz equation [42] $(\Delta_r+k_1^2)\mathcal{D}(\mathbf{r},\mathbf{r}',k_1) = \mathbf{I}\delta^{(3)}(\mathbf{r}-\mathbf{r}')$. $\tilde{\mathcal{D}}(\mathbf{r},\mathbf{r}',k_1)$ in Eq. (1) stands for a boundary term [42]. This function is a solution of the analogous homogeneous equation, and provides the necessary boundary conditions for $\mathbf{A}(\mathbf{r},k_1)$.

The Green function $\mathcal{D}(\mathbf{r},\mathbf{r}',k_1)$ can be expanded in multipoles [42]

$$\mathcal{D}(\mathbf{r},\mathbf{r}',k_1) = 4\pi i k_1 \sum_{J,M}\sum_{a=e,m} \mathcal{B}^a_{JM}(\mathbf{r},k_1)\mathcal{A}^{a^*}_{JM}(\mathbf{r}',k_1),$$

where $\mathcal{A}^{e,m}_{JM}$ and $\mathcal{B}^{e,m}_{JM}$ are the vector potentials of the electric (e) and magnetic (m) types $\mathcal{A}^e_{JM}(\mathbf{x},k) = \sum_{\nu=\pm1}(-1)^{1-\nu/2}\sqrt{[J+(1+\nu)/2]/(2J+1)}j_{J-\nu}(kx)\times \mathbf{Y}^{J-\nu}_{JM}(\Omega_{\mathbf{x}})$, $\mathcal{A}^m_{JM}(\mathbf{x},k) = j_J(kx)\mathbf{Y}^J_{JM}(\Omega_{\mathbf{x}})$, $\mathcal{B}^{e,m}_{JM}(\mathbf{x},k) = \mathcal{A}^{e,m}_{JM}(\mathbf{x},k)$ with $j_J(kx)\to h^{(1)}_J(kx)$. Here, $j_J(kx)$ and $h^{(1)}_J(kx)$ are the spherical Bessel function and spherical Hankel function of the first kind, respectively, $\mathbf{Y}^L_{JM}(\Omega) = \sum_{m,\sigma}C^{JM}_{Lm1\sigma}Y_{Lm}(\Omega)\mathbf{e}_\sigma$ stands for the vector spherical harmonics, $Y_{Lm}(\Omega)$ is the scalar spherical harmonic, $C^{JM}_{Lm1\sigma}$ is the Clebsch-Gordan coefficient, and $\mathbf{e}_\sigma$ is the spherical basis vector [43].

The function $\tilde{\mathcal{D}}(\mathbf{r},\mathbf{r}',k_1)$ must be regular at $\mathbf{r}=0$ and $\mathbf{r}'=0$ and symmetric in $\mathbf{r}\leftrightarrow\mathbf{r}'$. Therefore [42],

$$\tilde{\mathcal{D}}(\mathbf{r},\mathbf{r}',k_1) = 4\pi i k_1 \sum_{J,M}\sum_{a=e,m} \mathcal{R}^a_J\mathcal{A}^a_{JM}(\mathbf{r},k_1)\mathcal{A}^{a^*}_{JM}(\mathbf{r}',k_1),$$

where $\mathcal{R}^a_J$ is the reflection coefficient that must be chosen to satisfy the boundary conditions at the sphere at $r=R$.

The field $\mathbf{A}(\mathbf{r},k_2)$ outside the dielectric sphere is a divergent spherical wave. It can be written in the form analogous to Eq. (1) with the Green function [5]

$$\mathcal{D}(\mathbf{r},\mathbf{r}',k_2,k_1) = 4\pi i k_1 \sum_{J,M}\sum_{a=e,m} \mathcal{T}^a_J\mathcal{B}^a_{JM}(\mathbf{r},k_2)\mathcal{A}^{a^*}_{JM}(\mathbf{r}',k_1),$$

where $\mathcal{T}^a_J$ is the transmission coefficient.

Using the multipole expansions for $\mathcal{D}(\mathbf{r},\mathbf{r}',k_1)$, $\tilde{\mathcal{D}}(\mathbf{r},\mathbf{r}',k_1)$, and $\mathcal{D}(\mathbf{r},\mathbf{r}',k_2,k_1)$, we can write the fields in the form $\mathbf{A}(\mathbf{r},k_{1(2)}) = \sum_{J,M}\sum_{a=e,m}\mathbf{A}^a_{JM}(\mathbf{r},k_{1(2)})$. The isomeric nuclear transition $3/2^+(7.8\text{ eV}) \to 5/2^+(0.0)$ in the ^{229}Th nucleus is a magnetic dipole ($M1$) transition with a negligible $E2$ component [44] [even for the magnitude of the reduced probability of the $E2$ nuclear transition $B_{W.u.}(E2)\simeq 100$, the probabilities of the $E2$ and $M1$ photon emission obey the relation $W_\gamma(E2)/W_\gamma(M1)\lesssim 10^{-9}$]. Therefore, in the sums over the multipoles, we can leave the term corresponding to the magnetic vector potential with a fixed value of J and obtain

$$\mathbf{A}^m_{JM}(\mathbf{r},k_1) = [h^{(1)}_J(k_1r) + \mathcal{R}^m_J j_J(k_1r)]\mathbf{Y}^J_{JM}(\Omega_{\mathbf{r}})\langle\mathcal{N}^m_{JM}\rangle$$
$$\mathbf{A}^m_{JM}(\mathbf{r},k_2) = \mathcal{T}^m_J h^{(1)}_J(k_2r)\mathbf{Y}^J_{JM}(\Omega_{\mathbf{r}})\langle\mathcal{N}^m_{JM}\rangle, \qquad (2)$$

where we have used the notation $\langle\mathcal{N}^m_{JM}\rangle = 4\pi i k_1\times \int \mathcal{A}^{m^*}_{JM}(\mathbf{r}',k_1)\cdot\mathbf{J}(\mathbf{r}')d^3r'$. The electric and magnetic fields corresponding to the potentials $\mathbf{A}^m_{JM}(\mathbf{r},k_{1,2})$ are defined as $\mathbf{E}^m_{JM}(t,\mathbf{r},k) = i\omega\mathbf{A}^m_{JM}(t,\mathbf{r},k)$, $\mathbf{B}^m_{JM}(t,\mathbf{r},k) = ik\mathbf{A}^e_{JM}(t,\mathbf{r},k)$.

The reflection coefficient $\mathcal{R}^m_J$, which has the form [5]

$$\mathcal{R}^m_J = \frac{\sqrt{\varepsilon_1}\xi'_J(\rho_1)\xi_J(\rho_2) - \sqrt{\varepsilon_2}\xi_J(\rho_1)\xi'_J(\rho_2)}{\sqrt{\varepsilon_2}\psi_J(\rho_1)\xi'_J(\rho_2) - \sqrt{\varepsilon_1}\psi'_J(\rho_1)\xi_J(\rho_2)}, \qquad (3)$$

obtained from the boundary conditions for the tangential components of electric and magnetic fields at the media interface, $\mathbf{E}^m_{JM_\parallel}(R,k_1) = \mathbf{E}^m_{JM_\parallel}(R,k_2)$, $\mathbf{B}^m_{JM_\parallel}(R,k_1) = \mathbf{B}^m_{JM_\parallel}(R,k_2)$. In Eq. (3), $\psi_J(x) = xj_J(x)$ and $\xi_J(x) = xh^{(1)}_J(x)$ are the Riccati-Bessel functions, $\rho_{1(2)} = k_{1(2)}R$.

The Purcell factor f_P is the ratio of the transition probability from a source located near the interface and the probability in an infinite medium. For the $M1$ radiation source located at the center of the sphere, the Purcell factor is calculated by the formula [6]:

$$f_P^{M1} = 1 + \mathrm{Re}[\mathcal{R}^m_1]. \qquad (4)$$

In addition, using the reflection coefficient, the corresponding frequency shift can also be estimated from the relation $\Delta\omega/\Gamma^{M1}_\gamma = \mathrm{Im}[\mathcal{R}^m_J]/2$ [6], where Γ^{M1}_γ is the $M1$ γ emission probability in an infinite medium.

The influence of the boundary conditions on the $M1(7.8\text{ eV})$ γ transition is demonstrated in Figs. 1–2. As a host, we consider a crystal with a band gap larger than ω. This can be, for example, $LiSrAlF_6$, which is easily doped with ^{229}Th and has the refractive index $n=\sqrt{\varepsilon}\approx 1.4$–$1.5$ at $\omega\approx 8$ eV. For Al, we obtain $\varepsilon = -2.8 + i0.30$ at $\omega\approx 8$ eV [45].

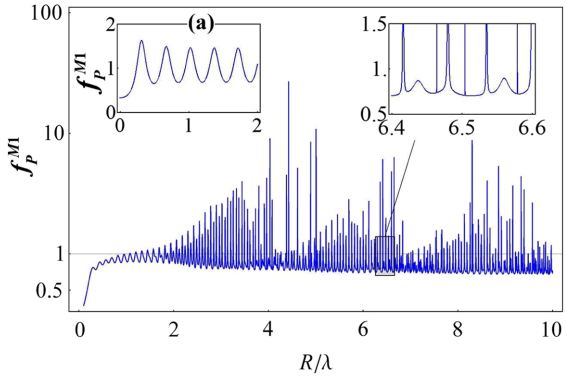

FIG. 1. The averaged Purcell factor $\langle f_P^{M1}\rangle$ (6) for the ^{229}Th nuclei uniformly distributed inside a dielectric sphere as a function of R/λ. The inset (a) shows f_P^{M1} for the ^{229}Th nuclei placed at the center of a sphere.

As follows from Figs. 1(a)–2(a), the γ emission probability can vary by a factor of 1.5 due to the presence of the $LiSrAlF_6$/vacuum boundary. If a dielectric sphere is placed in the Al cavity, the decay rate can vary by a factor of 50–60. This is a consequence of the high reflectivity of aluminum at $\omega = 8$ eV. As for the normalized frequency shift, its value oscillates as a function of R/λ in the range $|\Delta\omega/\Gamma_\gamma^{M1}| \leq 0.2$ for a dielectric sphere in a vacuum, and in the range $|\Delta\omega/\Gamma_\gamma^{M1}| \leq 10$ for a dielectric in a cavity of metallic Al.

The present consideration can be easily generalized to the case of a dielectric microsphere filled with ^{229}Th with the distribution $n(r'_N)$. To calculate the radiation probability (4) in the case when the nucleus is located at a distance $0 < r'_N < R$ from the center of the sphere, the current in the form $\mathbf{J}(\mathbf{r}') = \mathbf{J}_0\delta(\mathbf{r}' - \mathbf{r}'_N)$ is substituted in Eq. (1). Following the work of [2–4,7], we obtain formulas for the Purcell factors for a magnetic dipole oriented in the radial ($\perp$) and tangential ($\|$) directions

$$f_{P_\perp}^{M1} = 1 + \frac{3}{2}\sum_{J=1}^{\infty} J(J+1)(2J+1)\frac{j_J^2(y)}{y^2}\mathrm{Re}[\mathcal{R}_J^m],$$

$$f_{P_\parallel}^{M1} = 1 + \frac{3}{4}\sum_{J=1}^{\infty}(2J+1)\left(\frac{\psi'^2_J(y)}{y^2}\mathrm{Re}[\mathcal{R}_J^m] + j_J^2(y)\mathrm{Re}[\mathcal{R}_J^e]\right),$$

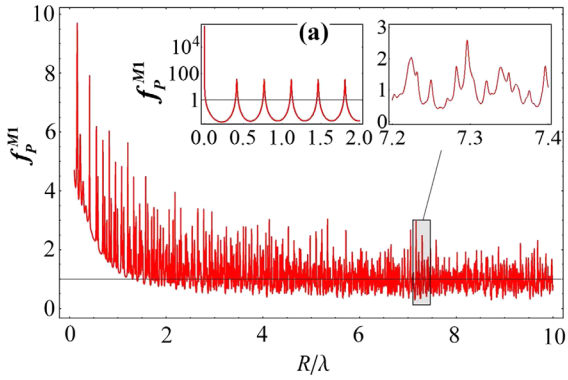

FIG. 2. The same as in Fig. 1, but with the dielectric sphere placed in a cavity of metallic Al.

where $y = k_1 r'_N$, $\mathcal{R}_J^e$ is the reflection coefficient for electric multipoles (TM mode), which is connected with $\mathcal{R}_J^m$ by the relation $\mathcal{R}_J^e = \mathcal{R}_J^m$ with $\varepsilon_{1,2} \to \varepsilon_{2,1}$. When $r'_N \to 0$, only the term with $J = 1$ remains in the sum, and we arrive at Eq. (4).

The total Purcell factor $f_P^{M1} = (1/3)f_{P_\perp}^{M1} + (2/3)f_{P_\parallel}^{M1}$ depends on the distance to the center of the sphere r'_N. Accordingly, the γ decay of nuclei located in the different spherical layers occurs at different rates. The detector, in turn, measures the decay activity $Q(t)$ from the entire source:

$$Q(t) = \int_V \lambda(r'_N)n(r'_N)e^{-\lambda(r'_N)t}dV, \tag{5}$$

where $\lambda(r'_N) = f_P^{M1}(r'_N)\lambda_0$ is the decay constant of the nuclei placed in the corresponding spherical layer, $\lambda_0 = \Gamma_\gamma^{M1}$, and $n(r'_N)$ is the density of the nuclei distribution. The presence of the Purcell factor in the exponent in Eq. (5) means that the averaged activity as a function of time can differ markedly from the exponential one (see below).

To get an idea of the decay rate in a distributed source at the initial time, one can average the Purcell factor over the volume of the dielectric sphere V. The averaging of f_P^{M1} is carried out using the uniform distribution of sources $n(r'_N) = (4\pi R^3/3)^{-1}$. Integration $\int_V f_P^{M1}(r'_N)n(r'_N)d^3r'_N$ (see Ref. [4] for details) gives the following formula for the normalized average decay probability at $t = 0$

$$\langle f_P^{M1}\rangle = 1 + \frac{3}{4}\sum_{J=1}^{\infty}(2J+1)\Big[(j_J^2(\rho_1) - j_{J-1}(\rho_1) \times j_{J+1}(\rho_1))\mathrm{Re}[\mathcal{R}_J^e] + \Big(j_{J-1}^2(\rho_1) - \frac{2J-1}{\rho_1} \times j_{J-1}(\rho_1)j_J(\rho_1) + \frac{\rho_1^2 - 2J}{\rho_1^2}j_J^2(\rho_1)\Big)\mathrm{Re}[\mathcal{R}_J^m]\Big]. \tag{6}$$

An example of a calculation is given in Figs. 1–2. The main feature of Fig. 1 is the appearance of narrow high peaks. They emerge as a result of the total internal reflection of the electromagnetic waves emitted parallel to the media interface by the sources placed near the interface. The corresponding standing waves create strong electromagnetic fields at certain locations inside the dielectric sphere, which lead to the acceleration of the isomeric nuclei decay. The peaks disappear if the refractive index of the dielectric medium surrounding the sphere satisfies the condition $n_2 > n_1$. Note that this situation is very similar to the $E1$ atomic radiation in water drops of micron size described in detail in Ref. [4].

Gamma emission in the dielectric thin film.—Let us consider the decay of the ^{229}Th nuclei, which can be excited in a laser plasma [44] and implanted in the form of the Th ions into the thin (with the width $d_0 \simeq 10$ nm) SiO_2 film (the band gap is $\simeq$10 eV) grown on the Si substrate [46].

The Purcell factor at the case of the $M1$ radiation is obtained by generalizing the approach [47] for the $E1$ transition. The calculation gives:

$$f_P^{M1}(z) = \frac{1}{2}\mathrm{Im}\int_0^\infty \left\{ \frac{F(\hat{d}_0-\hat{z},R_{12}^{\perp})F(\hat{z},R_{13}^{\perp})}{F(\hat{d}_0,-R_{12}^{\perp}R_{13}^{\perp})}\frac{\kappa^3}{l_1} + \left[(1-\kappa^2)\frac{F(\hat{d}_0-\hat{z},-R_{12}^{\perp})F(\hat{z},-R_{13}^{\perp})}{F(\hat{d}_0,-R_{12}^{\perp}R_{13}^{\perp})} + \frac{F(\hat{d}_0-\hat{z},-R_{12}^{\parallel})F(\hat{z},-R_{13}^{\parallel})}{F(\hat{d}_0,-R_{12}^{\parallel}R_{13}^{\parallel})}\right]\frac{\kappa}{l_1}\right\} d\kappa. \quad (7)$$

Here, $F(x,y) = 1 + y\exp(-2l_1x)$, $\hat{d}_0 = k_1 d_0$, $\hat{z} = k_1 z$, and z is the distance between the ^{229}Th nuclei and vacuum/SiO_2 interface. The reflection coefficients in Eq. (7) are defined as $R_{1,j}^{\parallel} = (\varepsilon_1 l_j - \varepsilon_j l_1)/(\varepsilon_1 l_j + \varepsilon_j l_1)$, $R_{1,j}^{\perp} = (\varepsilon_1 - \varepsilon_j)/(\varepsilon_1 + \varepsilon_j)$, where $l_1 = -i\sqrt{1-\kappa^2}$, $j = 2$, 3, $l_j = -i\sqrt{\varepsilon_j/\varepsilon_1 - \kappa^2}$, index 1 refers to SiO_2, index 2 to Si, and index 3 to the vacuum.

As far as f_P^{M1} is dependent on the position of the emitting object relative to the interfaces, we calculated f_P^{M1} as a function of z for the following values of dielectric constants: $\varepsilon_1 \approx 3.3$, $\varepsilon_2 = -3.6 + i1.9$ at the photons energy 8 eV. The result is shown in Fig. 3.

The radioactive decay curves for the same number N_0 of isomeric nuclei ^{229}Th uniformly distributed $[n(z) = N_0/d_0]$ in the SiO_2 thin film and placed in the infinite SiO_2 medium, are shown in Fig. 3. The curves are normalized to the initial activity in the infinite SiO_2 medium. It can be seen that the Purcell factor and decay probability for the nuclei placed in the vicinity of the SiO_2/Si interface are rather high. That is why at the initial time the activity of the nuclei in the film is higher than in the medium. Over time, the activity in the film decreases and then the decay is supported by nuclei located near the SiO_2/vacuum interface where $f_P^{M1} < 1$. All this leads to a seemingly nonexponential decay in the thin film.

Internal conversion in metal cavity.—Now we consider the decay of the ^{229}Th nuclear isomer in a spherical metal cavity. Here the dominant decay channel is the IC.

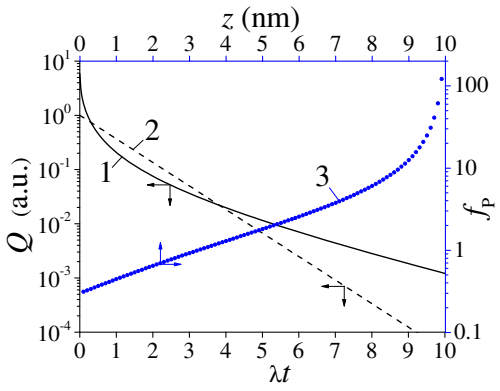

FIG. 3. Radioactive decay curves $Q(t)$ from Eq. (5) for the ^{229}Th nuclei in the SiO_2 thin film: (1) with $f_P^{M1}(z)$ for the SiO_2/Si sample from Eq. (7), (2) with $f_P^{M1}(z) = 1$, and (3) the Purcell factor $f_P^{M1}(z)$.

In the geometry under consideration, the change in the probability of the IC due to the influence of the metal cavity on the conversion electrons will be negligibly small. The energy of the conversion electrons during the decay of the ^{229}Th isomer is several electron volts. The normal incidence reflection coefficient of these electrons does not exceed 20% for Al [48]. The wavelength of such electrons is of the order of 10 Å. This is two orders of magnitude smaller than the wavelength of the nuclear transition and the cavity size, and it is comparable with the surface roughness of a high-quality cavity. As a result, electrons are scattered by the cavity surface, and there will be no quantum electronic states and effective interference of the incident and reflected electron waves. Therefore, this cavity can not significantly affect the density of the final states of conversion electrons.

Let us consider now the effect of a vacuum-metal interface on the IC in the ^{229}Th nucleus using the technique of the photon propagator. The Hamiltonian of the interaction of the electron current $\mathbf{j}(\mathbf{r})$ with the field $\mathbf{A}_{JM}^m(\mathbf{r},k_1)$ in Eq. (2) is $H_{\mathrm{int}} = \int \mathbf{j}(\mathbf{r})\mathbf{A}_{JM}^m(\mathbf{r},k_1)d^3r$. It is easy to see that the change in the rate of the IC decay of ^{229}Th is caused by a change of the electronic matrix element

$$\int \mathbf{j}(\mathbf{r})\cdot[\boldsymbol{\mathcal{B}}_{JM}^m(\mathbf{r},k_1) - \mathcal{R}_J^m \boldsymbol{\mathcal{A}}_{JM}^m(\mathbf{r},k_1)]d^3r. \quad (8)$$

Taking into account that $h_J^{(1)}(y) = j_J(y) + in_J(y)$, where $n_J(y)$ is the spherical Neumann function, the radial part in Eq. (8) is represented by $\tilde{\mathsf{m}}_J^m(k_1) = (1-\mathcal{R}_J^m)\langle f|j_J(k_1r)|i\rangle + i\langle f|n_J(k_1r)|i\rangle$, where $|i\rangle$ and $|f\rangle$ are the initial and final radial wave functions of the electron.

The ratio of the IC probabilities for the nuclear MJ transition in a sphere and in vacuum is

$$f_{P_{IC}}^{MJ} = |\tilde{\mathsf{m}}_J^m(k_1)|^2/|\mathsf{m}_J^m(k_1)|^2, \quad (9)$$

where $\mathsf{m}_J^m(k_1) = \langle f|j_J(k_1r)|i\rangle + i\langle f|n_J(k_1r)|i\rangle$. Using the dimensionless parameter $\delta_J = \langle f|j_J(k_1r)|i\rangle/\langle f|n_J(k_1r)|i\rangle$, we rewrite Eq. (9) as

$$f_{P_{IC}}^{MJ} = \frac{1 + 2\mathrm{Im}[\mathcal{R}_J^m]\delta_J + [(1+\mathrm{Re}[\mathcal{R}_J^m])^2 + (\mathrm{Im}[\mathcal{R}_J^m])^2]\delta_J^2}{1+\delta_J^2}.$$

In the case of low-energy nuclear transitions, we have $\delta_J \ll 1$. For example, the numerical calculation yields $\delta_1 \le 10^{-14}$ for the $M1$ IC from the $7s_{1/2}$ shell of the Th atom. At the same time, the imaginary and real parts of the reflection coefficient $\mathcal{R}_1^m$ for metallic Al are $\{|\mathrm{Re}[\mathcal{R}_1^m]|, |\mathrm{Im}[\mathcal{R}_1^m]|\} \le 1$ in the range $x \ge 1$. The similar situation holds for the $E2$ component of the $3/2^+(7.8\ \mathrm{eV}) \to 5/2^+(0.0)$ transition: $\delta_2 \simeq 10^{-14} - 10^{-15}$ for the $E2$ IC from the $6d_{3/2}$ shell and $\delta_2 \simeq 10^{-12} - 10^{-14}$ for the transitions from the $7s_{1/2}$ shell, and $\{|\mathrm{Re}[\mathcal{R}_2^e]|, |\mathrm{Im}[\mathcal{R}_2^e]|\} \le 1$ in the range $x \ge 1$. Thus, $f_{P_{IC}}^{M1} \simeq 1$, and inside a metal cavity it is not possible to detect a visible change in the probability of the IC for the ^{229}Th isomeric transition.

The electronic wave functions corresponding to a bound state are localized in the region $r \lesssim a_B$ in the IC process,

where a_B is the Bohr radius, and all electron integrations should be performed in this region. However, in this region, the argument of the spherical functions $j_J(\omega r)$ and $n_j(\omega r)$ in the matrix element $\mathsf{m}_J^m(k_1)$ satisfies the condition $\omega a_B \ll 1$. The Bessel function $j_J(\omega r) \sim (\omega r)^J$ is very small, while the Neumann function has a pole $n_J(\omega r) \sim 1/(\omega r)^{J+1}$. Correspondingly, the imaginary part of the matrix element $\mathsf{m}_J^m(k_1)$ is several orders of magnitude larger than the real part, and $\delta_J \ll 1$.

In the IC process for the $M1$ component, the atomic nucleus and the electron exchange a virtual photon, whose energy is $\omega = 7.8$ eV, and the momentum is $q = p_f = \sqrt{2mE}$. Here, p_f is the momentum of the electron in the final state, m is the electron mass, and $E = \omega + E_b$ is the energy of the conversion electron, whose initial atomic shell binding energy is E_b. For the conversion from the $7s_{1/2}$ state, $E_b \approx -6$ eV, $E \approx 2$ eV and $q \approx 1.5 \times 10^3$ eV. Such a virtual photon lies outside the mass surface. It has an effective "mass" $m_\gamma^* = \sqrt{q^2 - \omega^2} \simeq q$, exists for a time of the order $\Delta t \simeq 1/m_\gamma^* \approx 4 \times 10^{-19}$ s, and it provides an effective interaction of the characteristic length $r_\gamma \leq \Delta t \simeq 1/m_\gamma^* \approx 10^{-8}$ cm, which is much less than the cavity radius $R \geq \lambda = 2\pi/\omega = 1.6 \times 10^{-5}$ cm. Thus, the virtual photon attenuates at very short distances, and the resultant reflected wave is very weak. It should be noted that for the same reason, it does not matter where the atom is located inside the cavity.

Summing up, we have shown the possibility to control the radioactive decay of the isomeric ^{229}Th nuclei due to the boundary conditions for the electromagnetic field. This can be important for experimental studies of the isomeric level properties, in particular for obtaining realistic values of the isomer half-life and nuclear transition matrix element.

This research was supported by a grant of the Russian Science Foundation (Project No 16-12-00001).

*tkalya@srd.sinp.msu.ru

[1] E. M. Purcell, Phys. Rev. **69**, 681 (1946).
[2] K. Ohtaka and A. A. Lucas, Phys. Rev. B **18**, 4643 (1978).
[3] H. Chew, J. Chem. Phys. **87**, 1355 (1987).
[4] H. Chew, Phys. Rev. A **38**, 3410 (1988).
[5] H. Ajiki, T. Tsuji, K. Kawano, and K. Cho, Phys. Rev. B **66**, 245322 (2002).
[6] K. G. Sullivan and D. G. Hall, Phys. Rev. A **50**, 2708 (1994).
[7] V. V. Klimov and V. S. Letokhov, Laser Phys. **15**, 61 (2005).
[8] P. Goy, J. M. Raimond, M. Gross, and S. Haroche, Phys. Rev. Lett. **50**, 1903 (1983).
[9] H. Schniepp and V. Sandoghdar, Phys. Rev. Lett. **89**, 257403 (2002).
[10] P. Anger, P. Bharadwaj, and L. Novotny, Phys. Rev. Lett. **96**, 113002 (2006).
[11] L. Aigouy, A. Caze, P. Gredin, M. Mortier, and R. Carminati, Phys. Rev. Lett. **113**, 076101 (2014).
[12] A. E. Krasnok, A. P. Slobozhanyuk, C. R. Simovski, S. A. Tretyakov, A. N. Poddubny, A. E. Miroshnichenko, Y. S. Kivshar, and P. A. Belov, Sci. Rep. **5**, 12956 (2015).
[13] J. P. Hannon and G. T. Trammell, Hyperfine Interact. **123/124**, 127 (1999).
[14] L. A. Kroger and C. W. Reich, Nucl. Phys. **A259**, 29 (1976).
[15] C. W. Reich and R. G. Helmer, Phys. Rev. Lett. **64**, 271 (1990).
[16] R. G. Helmer and C. W. Reich, Phys. Rev. C **49**, 1845 (1994).
[17] B. R. Beck, J. A. Becker, P. Beiersdorfer, G. V. Brown, K. J. Moody, J. B. Wilhelmy, F. S. Porter, C. A. Kilbourne, and R. L. Kelley, Phys. Rev. Lett. **98**, 142501 (2007).
[18] L. von der Wense *et al.*, Nature (London) **533**, 47 (2016).
[19] E. Browne, E. B. Norman, R. D. Canaan, D. C. Glasgow, J. M. Keller, and J. P. Young, Phys. Rev. C **64**, 014311 (2001).
[20] T. Mitsugashira, M. Hara, T. Ohtsuki, H. Yuki, K. Takamiya, Y. Kasamatsu, A. Shinohara, H. Kikunaga, and T. Nakanishi, J. Radioanal. Nucl. Chem. **255**, 63 (2003).
[21] H. Kikunaga, Y. Kasamatsu, H. Haba, T. Mitsugashira, M. Hara, K. Takamiya, T. Ohtsuki, A. Yokoyama, T. Nakanishi, and A. Shinohara, Phys. Rev. C **80**, 034315 (2009).
[22] T. T. Inamura and H. Haba, Phys. Rev. C **79**, 034313 (2009).
[23] A. Yamaguchi, M. Kolbe, H. Kaser, T. Reichel, A. Gottwald, and E. Peik, New J. Phys. **17**, 053053 (2015).
[24] J. Jeet, C. Schneider, S. T. Sullivan, W. G. Rellergert, S. Mirzadeh, A. Cassanho, H. P. Jenssen, E. V. Tkalya, and E. R. Hudson, Phys. Rev. Lett. **114**, 253001 (2015).
[25] E. V. Tkalya, JETP Lett. **71**, 311 (2000).
[26] E. V. Tkalya, A. N. Zherikhin, and V. I. Zhudov, Phys. Rev. C **61**, 064308 (2000).
[27] W. G. Rellergert, D. DeMille, R. R. Greco, M. P. Hehlen, J. R. Torgerson, and E. R. Hudson, Phys. Rev. Lett. **104**, 200802 (2010).
[28] M. P. Hehlen, R. R. Greco, W. G. Rellergert, S. T. Sullivan, D. DeMille, R. A. Jackson, E. R. Hudson, and J. R. Torgerson, J. Lumin. **133**, 91 (2013).
[29] P. Dessovic, P. Mohn, R. A. Jackson, G. Winkler, M. Schreitl, G. Kazakov, and T. Schumm, J. Phys. Condens. Matter **26**, 105402 (2014).
[30] S. Stellmer, M. Schreitl, and T. Schumm, Sci. Rep. **5**, 15580 (2015).
[31] E. Peik and C. Tamm, Europhys. Lett. **61**, 181 (2003).
[32] C. J. Campbell, A. V. Steele, L. R. Churchill, M. V. DePalatis, D. E. Naylor, D. N. Matsukevich, A. Kuzmich, and M. S. Chapman, Phys. Rev. Lett. **102**, 233004 (2009).
[33] C. J. Campbell, A. G. Radnaev, A. Kuzmich, V. A. Dzuba, V. V. Flambaum, and A. Derevianko, Phys. Rev. Lett. **108**, 120802 (2012).
[34] E. V. Tkalya, JETP Lett. **55**, 211 (1992).
[35] S. G. Porsev, V. V. Flambaum, E. Peik, and C. Tamm, Phys. Rev. Lett. **105**, 182501 (2010).
[36] E. V. Tkalya, Phys. Rev. Lett. **106**, 162501 (2011).
[37] G. A. Kazakov, A. N. Litvinov, V. I. Romanenko, L. P. Yatsenko, A. V. Romanenko, M. Schreitl, G. Winkler, and T. Schumm, New J. Phys. **14**, 083019 (2012).

[38] E. Peik and M. Okhapkin, C.R. Phys. **16**, 516 (2015).
[39] V. V. Flambaum, Phys. Rev. Lett. **97**, 092502 (2006).
[40] E. V. Tkalya, Phys. Rev. A **94**, 012510 (2016).
[41] A. M. Dykhne, N. V. Eremin, and E. V. Tkalya, JETP Lett. **64**, 345 (1996).
[42] T. H. Hansson and R. L. Jaffe, Phys. Rev. D **28**, 882 (1983).
[43] D. A. Varshalovich *et al.*, *Quantum Theory of Angular Momentum* (World Sci. Publ., London, 1988).
[44] V. F. Strizhov and E. V. Tkalya, Sov. Phys. JETP **72**, 387 (1991).
[45] H. Ehrenreich, H. R. Philipp, and B. Segall, Phys. Rev. **132**, 1918 (1963).
[46] P. V. Borisyuk *et al.*, arXiv:1711.03378.
[47] R. R. Chance, A. Prock, and R. Silbey, Adv. Chem. Phys. **37**, 1 (1978).
[48] J. Cazaux, J. Appl. Phys. **111**, 064903 (2012).